Towards single molecule detection using photoacoustic microscopy

Amy M. Winkler, Konstantin Maslov, Lihong V. Wang

Amy M. Winkler, Konstantin Maslov, Lihong V. Wang, "Towards single molecule detection using photoacoustic microscopy," Proc. SPIE 8581, Photons Plus Ultrasound: Imaging and Sensing 2013, 85811A (4 March 2013); doi: 10.1117/12.2004265

SPIE.

Event: SPIE BiOS, 2013, San Francisco, California, United States

Towards single molecule detection using photoacoustic microscopy

Amy M. Winkler[a], Konstantin Maslov[a], Lihong V. Wang[*a]
[a]Department of Biomedical Engineering, Washington University in St. Louis, Whitaker Hall, One Brookings Dr., St. Louis, MO USA 63130

ABSTRACT

Recently, a number of optical imaging modalities have achieved single molecule sensitivity, including photothermal imaging, stimulated emission microscopy, ground state depletion microscopy, and transmission microscopy. These optical techniques are based on optical absorption contrast, extending single-molecule detection to non-fluorescent chromophores. Photoacoustics is a hybrid technique that utilizes optical excitation and ultrasonic detection, allowing it to scale both the optical and acoustic regimes with 100% sensitivity to optical absorption. However, the sensitivity of photoacoustics is limited by thermal noise, inherent in the medium itself in the form of acoustic black body radiation. In this paper, we investigate the molecular sensitivity of photoacoustics in the context of the thermal noise limit. We show that single molecule sensitivity is achievable theoretically at room temperature for molecules with sufficiently fast relaxation times. Hurdles to achieve single molecule sensitivity in practice include development of detection schemes that work at short working distance, <100 microns, high frequency, >100 MHz, and low loss, <10 dB.

Keywords: photoacoustic, microscopy, single molecule, thermal noise, acoustic black body radiation

1. INTRODUCTION

Photoacoustic tomography has been drawing the attention of the biomedical imaging community in the last decade [1]. A cross-over between optical imaging and ultrasound imaging, photoacoustics harnesses both the exquisite molecular contrast of optical absorption and the low scattering of ultrasound. Clinically, photoacoustic tomography is being used to add optical contrast to ultrasound imaging of breast cancer, due to its ability to image with acoustic resolution at depths beyond the optical diffusion limit, down to 2 cm demonstrated *in vivo* [2] and 8 cm in tissue phantoms [3], while retaining specific molecular sensitivity from optical absorption. Photoacoustics has also proven to be a highly scalable technique, achieving subcellular resolution within a millimeter depth of tissue [1, 4, 5]. Since the photoacoustic effect involves the transduction of light energy into sound energy, photoacoustic images are largely background free and present 100% sensitivity to optical absorption [6]. The high imaging contrast of photoacoustics has enabled quantification of a number of vascular metrics, including total hemoglobin concentration (C_{Hb}), blood oxygen saturation (sO_2), flow speed or volumetric flow rate, capillary density, metabolic rate of oxygen (MRO_2), and pulse wave velocity (PWV) [7, 8]. Furthermore, nonlinear effects have enabled ultrasharp spectroscopy [9] and even sub-diffraction imaging with spatial resolution <100 nm [10], making photoacoustic imaging the only optical imaging technique to break through both the optical diffusion and optical diffraction limits. At the sub-diffraction scale, however, the achievable resolution is limited by sensitivity as the number of molecules within a resolvable voxel becomes very small; for example, a 10 nm cube contains only 3 hemoglobin molecules at the corpuscular concentration, i.e. the concentration within a red blood cell.

Recently, a number of absorption-sensitive optical techniques have achieved single molecule sensitivity at room temperature, including photothermal [11], stimulated emission [12], ground state depletion [13], and transmission microscopy [14]. In this paper, we discuss the challenges in achieving a similar sensitivity using photoacoustic microscopy and estimate the sensitivity with optimum illumination and state-of-the-art acoustic detectors to be between 10s and 1000s of molecules, depending on the molecule.

* e-mail: lhwang@biomed.wustl.edu

Photons Plus Ultrasound: Imaging and Sensing 2013, edited by Alexander A. Oraevsky, Lihong V. Wang,
Proc. of SPIE Vol. 8581, 85811A · © 2013 SPIE · CCC code: 1605-7422/13/$18 · doi: 10.1117/12.2004265

2. THEORY

2.1. Photoacoustic Signal

Photocoustics is sensitive to the rapid deposition of heat due to optical absorption. In order to maximize our signal, we must consider how rapidly a single molecule can generate heat. Molecules have a finite relaxation time which ultimately limits the amount of heat deposited, or equivalently the number of photons absorbed, in a given time interval. The rate of heat deposition, $H(t)$, follows the formula for absorption saturation, described in laser theory [15].

$$H(t) = \eta\sigma I(t) / \left(1 + \frac{bI(t)}{I_{sat}}\right) \tag{1}$$

where η is the fraction of absorbed energy released as heat, σ is the absorption cross-section, $I(t)$ is the optical intensity, I_{sat} is the saturation intensity, and b is a factor of 1 or 2 depending on the electronic energy states of the molecule. In the Fourier domain, absorption saturation induces harmonics for $I(t) = I_0\left(1 + \cos(2\pi f_o t)\right)$, and the harmonic amplitudes, H_n, are given by:

$$H_n = 2f_o \int_{-1/2f_o}^{1/2f_o} \left(\frac{\eta\sigma b I_0(1+\cos(2\pi f_o t))}{1+bI_0(1+\cos(2\pi f_o t))/I_{\text{sat}}}\right) \cos(n2\pi f_o t)\mathrm{dt} = \frac{2\eta\sigma I_{\text{sat}}}{b\sqrt{1+2bI_0/I_{\text{sat}}}} \left(\frac{\sqrt{1+2bI_0/I_{\text{sat}}} - (1+bI_0/I_{\text{sat}})}{bI_0/I_{\text{sat}}}\right)^n, \; n \geq 1. \tag{2}$$

This explicit solution was found in [16]. For H_1, the peak occurs at $I_0 \approx 2.4b^{-1}I_{\text{sat}}$ and the peak value is about $H_{1\,\text{peak}} \approx 0.34 \cdot \eta\sigma b^{-1} I_{\text{sat}}$.

Consider the Fourier domain solution in the linear case for a cubic source of dimension, a, using the Born approximation [17]:

$$\tilde{p}(f) = \frac{i\beta}{2C_p} \frac{e^{-i2\pi fz/v_s}}{z} f\tilde{H}(f)\mathrm{sinc}(2\pi fa/2v_s) \tag{3}$$

where β is the thermal expansion coefficient, v_s is the speed of sound, C_p is the specific heat at constant pressure, z is the distance from the center of the spherical absorber to the point of measurement, and $\tilde{H}(f)$ is the Fourier transform of $H(t)$.

A single molecule is small compared to the wavelength of sound and is therefore approximately an acoustic point source. By allowing $\frac{\pi fa}{v_s} \to 0$, we arrive at the equation for an acoustic point source:

$$\tilde{p}(f) = \frac{i\beta}{2C_p} \frac{e^{-i2\pi fz/v_s}}{z} f\tilde{H}(f). \tag{4}$$

To account for ultrasonic absorption in the medium, which becomes significant for large f, Eq. 4 can be modified to include the exponential attenuation term:

$$\tilde{p}(f) = \frac{i\beta}{2C_p} \frac{e^{-i2\pi fz/v_s}}{z} f\tilde{H}(f) e^{-\alpha f^{\gamma} z}. \tag{5}$$

The optimum acoustic frequency can be determined analytically by setting the derivative with respect to frequency equal to zero:

$$f_{\text{peak}} = \frac{1}{(\gamma\alpha z)^{1/\gamma}}. \tag{6}$$

In aqueous medium, the attenuation is $\alpha_{\text{water}} = 25 \cdot 10^{-15}$ Hz^{-2} m^{-1} and $\gamma_{\text{water}} = 2$. The optimum frequency for a giving imaging depth, z, is shown in Figure **1**.

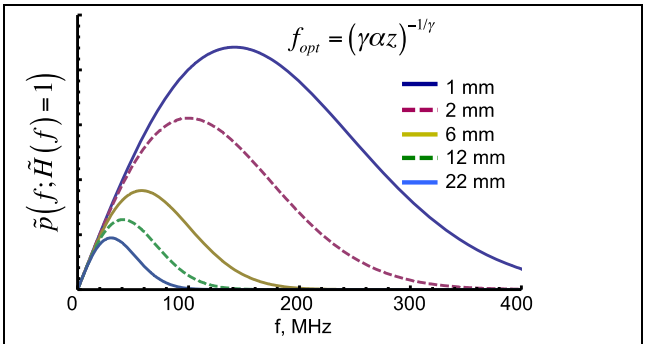

Figure 1: (color online) Pressure amplitude vs. frequency for various depth regimes in water.

The optimum regime for single molecule detection is clearly at shallow depth and at high frequency. This regime also facilitates tight optical focusing, meaning that optical intensities above the saturation intensity can be achieved for many molecules. For example, the saturation intensity of oxygenated hemoglobin in the Q-band of the absorption spectrum is 100 MW/cm^2 [18]. In the case of a Gaussian beam profile, a peak intensity of 500 MW/cm^2 can be achieved with 2 W incident power with beam waist 0.5 μm, achievable with commercially available continuous wave lasers and objective lenses.

Substituting $H_{1\,\mathrm{peak}} \approx 0.34 \cdot \eta\sigma b^{-1} I_{\mathrm{sat}}$ and $f_{\mathrm{peak}} = (\gamma\alpha z)^{-1/\gamma}$ into the equation for pressure amplitude, we arrive at an expression for the optimized pressure amplitude at the fundamental frequency, $|p_1|$, given by:

$$|p_1| = 0.17 \cdot \left(\frac{\beta e^{-1/\gamma}}{C_p(\gamma\alpha)^{1/\gamma}}\right)(\eta\sigma b^{-1} I_{\mathrm{sat}})\left(z^{-(1+1/\gamma)}\right). \tag{7}$$

Here, the expression for $|p_1|$ is grouped such that the first term in parentheses contains parameters related to the medium, the second term to the absorber, and the last term to the detector.

2.2. Acoustic Black Body Radiation

Thermal noise exists in the medium and can be detected by a transducer in the form of acoustic black body radiation [19]. The form of thermal noise is derived using the equal partition principle of statistical mechanics, which states that each degree of freedom contributes a noise energy equal to $\boldsymbol{k_B T}$, where $\boldsymbol{k_B}$ is the Boltzmann constant and $\boldsymbol{T}$ is temperature. Analogous to the derivation of black body radiation in optics, the power spectrum of thermal noise can be calculated by computing the number of degrees of freedom in a unit volume of temperature $\boldsymbol{T}$ and differentiating with respect to frequency, $\boldsymbol{f}$. The power spectrum of thermal noise radiation per unit area per unit solid angle, $\boldsymbol{U_n}$, is given by [19]:

$$U_n(f) = k_B T \cdot f^2 / {v_s}^2 \tag{8}$$

where v_s is the speed of sound. Here we assume that black body radiation condition is satisfied, i.e. that acoustic absorption in the media is sufficiently high, which is valid for a semi-infinite medium. This energy is radiated omnidirectionally; however, an acoustic detector only receives a fraction of this energy based on its etendue, ε. The etendue is defined in terms of the area of the detector, A, which we assume is uniform and not apodized, and the normalized directivity of the transducer, $D_n(\alpha, \beta)$.

$$\varepsilon = A \iint |D_n(\alpha,\beta)|^2 \, d\alpha d\beta \tag{9}$$

The theory of angular spectrum relates $D_n(\alpha, \beta)$ to the amplitude transmittance of the transducer, $t(x, y)$ [20]:

$$D_n(\alpha,\beta) = \iint t(x,y)\exp\left(j2\pi/\lambda(\alpha x+\beta y)\right)dxdy \Big/ \iint |t(x,y)|^2\,dxdy \tag{10}$$

where (α,β) are direction cosines, (x,y) is position on the transducer, and λ is the acoustic wavelength. For an unapodized transducer,

$$A = \iint |t(x,y)|^2\,dxdy. \tag{11}$$

Applying Parceval's theorem and substituting A for $\iint |t(x,y)|^2\,dxdy$ yields:

$$\iint |D_n(\alpha,\beta)|^2\,d\alpha d\beta = \lambda^2. \tag{12}$$

So ε of a diffraction-limited transducer is equal to λ^2 and the power spectrum of thermal noise received by the transducer, S_n, is given by:

$$S_n(f) = U_n(f)\cdot\lambda^2 = k_B T. \tag{13}$$

In order to be detectable even with an ideal detector, the power spectrum of the photoacoustic signal must be larger than $k_B T$. Cooling the medium to actually counterproductive in the case of photoacoustics since the thermal expansion coefficient, β, decreases with temperature. The power of the optimized photoacoustic signal at the fundamental frequency within a bandwidth df, S_s, is given by:

$$S_s(f=f_o)df = |p_1|^2 A/(2Z_a) = 0.014\cdot\left(\frac{\beta^2 e^{-\frac{2}{\gamma}}}{Z_a {C_p}^2(\gamma\alpha)^{\frac{2}{\gamma}}}\right)(\eta\sigma b^{-1} I_{\text{sat}})^2\left(z^{-2\left(1+\frac{1}{\gamma}\right)}A\right) \tag{14}$$

where Z_a is the characteristic acoustic impedance of the medium.

Here, again, we group terms into parameters related to the medium, absorber, and detector. The detector parameters can be written in terms of the numerical aperture, $NA^2 \approx A/(\pi z^2)$. In water, $\beta_{\text{water}} = 4\text{x}10^{-4}$ 1/K, $\gamma_{\text{water}} = 2$, $Z_{a\,\text{water}} =$ 1.5 MRayls/m^2, $C_{p\,\text{water}} = 4000$ J/kg/K, and $\alpha_{\text{water}} = 25\cdot 10^{-15}$ Hz^{-2} m^{-1}, so the acoustic power of an absorber in water is given by:

$$S_{s\,\text{water}}(f=f_o)df = (687\ \text{m/W})\cdot(\eta\sigma b^{-1} I_{\text{sat}})^2(\pi NA^2/z). \tag{15}$$

Figure 2 shows the acoustic powers and pressures generated from a single molecule of methylene blue (MB), oxygenated hemoglobin (HbO_2), and deoxygenated hemoglobin (HbR) as a function of working distance. At a bandwidth of 1 Hz, a single Hb molecule generates sufficient power to overcome acoustic thermal noise in the medium at a working distance of 1 mm. The optimum frequency at a 1 mm working distance is about 150 MHz, which presents a problem from a detection standpoint since most transducers that operate at this frequency are optimized from broadband detection and therefore exhibit more than 20 dB insertion loss. This loss directly reduces our molecular sensitivity and pushes the minimum detectable distance to around 10 μm, which is significantly more difficult to achieve.

The Q-band absorption properties of these three molecules is shown in Table **1** [18, 21]. Note that the optimized optical intensity only depends on the absorption lifetime, τ, and b. The acoustic power is calculated for a NA of 0.5.

Table 1: Properties of methylene blue (MB), oxygenated hemoglobin (HbO_2), and deoxygenated hemoglobin (HbR) at 532 nm.

Molecule	Lifetime, τ (picoseconds)	b	$\sigma b^{-1} I_{\text{sat}} = b^{-1}\cdot h\nu/\tau$ (nanowatts)
MB	380	1	1.0
HbO_2	22	1	17
HbR	2	1	190

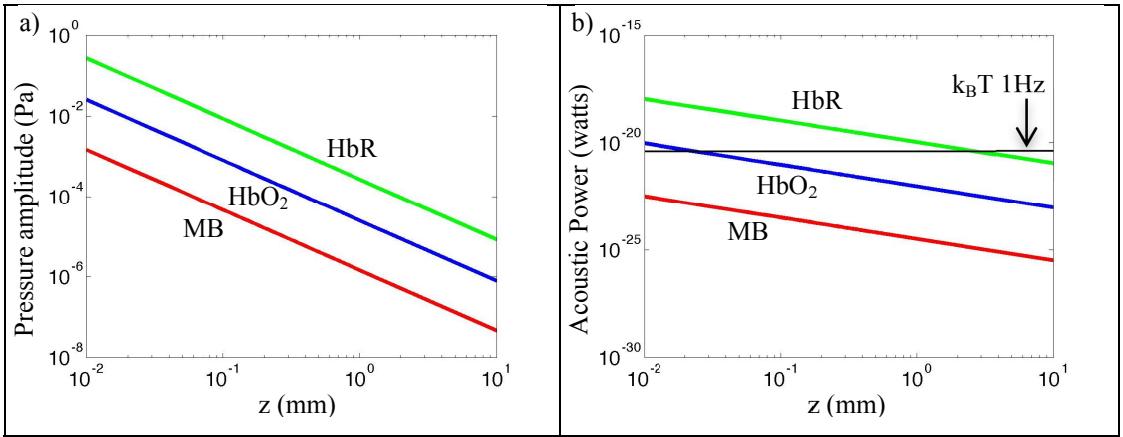

Figure 2: (color online) a) The optimum pressure amplitude in Pascals at the fundamental frequency as a function of working distance for methylene blue (MB), oxygenated hemoglobin (HbO_2), and deoxygenated hemoglobin (HbR). b) The optimum acoustic power in watts at the fundamental frequency for an NA of 0.5 as a function of working distance for MB, HbO_2, and HbR. The horizontal black line at around 10^{-21} watts indicates the acoustic noise due to thermal noise in the medium in a 1 Hz bandwidth.

3. MATERIALS AND METHODS

To test the theory, we built a continuous wave photoacoustic microscopy system. We utilized a 50 MHz transducer with a 6 mm working distance in water and losses of around 20 dB. The transducer losses should reduce our sensitivity in terms of number of molecules by about 10X. The bandwidth was limited using a lock-in-amplifier to 1.25 Hz. We measured the signal-to-noise ratio for 0.1%, 0.01%, and 0.001% methylene blue in a 12.7 μm thick mold and oxygenated hemoglobin within a monolayer of red blood cells with an average thickness of 2 μm as a function of incident optical intensity. After verifying linearity with respect to intensity, we extrapolated the noise equivalent number of molecules (NEM) by calculating the number of molecules in the voxel and dividing by the SNR at the highest optical intensity, which was 3% of the saturation intensity for both molecules. We then extrapolated to the NEM at the optimum intensity using our model.

4. RESULTS

We estimated an NEM of 186,000 methylene blue and 86,000 oxygenated hemoglobin molecules at 3% the saturation intensity in a 10% duty cycle of modulated continuous wave illumination. We extrapolated an NEM of 1500 methylene blue and 600 oxygenated hemoglobin molecules under optimum illumination conditions at the 6-mm working distance of our transducer. According to our model, we should have an NEM of 4000 methylene blue and 200 oxygenated hemoglobin molecules at a working distance of 6 mm with 20 dB transducer losses, which agrees with our measured value to within an order of magnitude.

5. CONCLUSION

We derived and verified the sensitivity of photoacoustic microscopy to number of molecules. Using a readily available ultrasonic transducer, we demonstrate a sensitivity of thousands of methylene blue molecules and hundreds of oxygenated hemoglobin molecules. In order to reach single molecule sensitivity, photoacoustic detectors that work with low loss (<10 dB insertion loss), shallow working distance (<1 mm), and high frequency (>100 MHz).

REFERENCES

[1] Wang, L. V. and Hu, S., "Photoacoustic Tomography: In Vivo Imaging from Organelles to Organs," Science 335(6075), 1458-1462 (2012).

[2] Ermilov, S. A., Khamapirad, T., Conjusteau, A., Leonard, M. H., Lacewell, R., Mehta, K., Miller, T. and Oraevsky, A. A., "Laser optoacoustic imaging system for detection of breast cancer," Journal of Biomedical Optics 14(2), 024007-024014 (2009).

[3] Ke, H., Erpelding, T. N., Jankovic, L., Liu, C. and Wang, L. V., "Performance characterization of an integrated ultrasound, photoacoustic, and thermoacoustic imaging system," Journal of Biomedical Optics 17(5), 056010-056016 (2012).

[4] Yao, D.-K., Maslov, K., Shung, K. K., Zhou, Q. and Wang, L. V., "In vivo label-free photoacoustic microscopy of cell nuclei by excitation of DNA and RNA," Opt. Lett. 35(24), 4139-4141 (2010).

[5] Zhang, C., Maslov, K. and Wang, L. V., "Subwavelength-resolution label-free photoacoustic microscopy of optical absorption in vivo," Opt. Lett. 35(19), 3195-3197 (2010).

[6] Wang, L. V., "Tutorial on Photoacoustic Microscopy and Computed Tomography," Selected Topics in Quantum Electronics, IEEE Journal of 14(1), 171-179 (2008).

[7] Yao, J., Maslov, K. I., Zhang, Y., Xia, Y. and Wang, L. V., "Label-free oxygen-metabolic photoacoustic microscopy in vivo," Journal of Biomedical Optics 16(7), 076003-076011 (2011).

[8] Yeh, C., Hu, S., Maslov, K. and Wang, L. V., "Photoacoustic microscopy of blood pulse wave," Journal of Biomedical Optics 17(7), 070504-070503 (2012).

[9] Zharov, V. P., "Ultrasharp nonlinear photothermal and photoacoustic resonances and holes beyond the spectral limit," Nat Photon 5(2), 110-116 (2011).

[10] Danielli, A., Maslov, K., Garcia-Uribe, A., Winkler, A. M., Li, C., Wang, L., Zhang, Y. S. and Wang, L. V., "Non-linear photoacoustic microscopy with optical sectioning," Oral Presentation at SPIE Bios Photonics West BO302-89, San Francisco, CA, (2013).

[11] Gaiduk, A., Yorulmaz, M., Ruijgrok, P. V. and Orrit, M., "Room-Temperature Detection of a Single Molecule's Absorption by Photothermal Contrast," Science 330(6002), 353-356 (2010).

[12] Min, W., Lu, S., Chong, S., Roy, R., Holtom, G. R. and Xie, X. S., "Imaging chromophores with undetectable fluorescence by stimulated emission microscopy," Nature 461(7267), 1105-1109 (2009).

[13] Chong, S., Min, W. and Xie, X. S., "Ground-State Depletion Microscopy: Detection Sensitivity of Single-Molecule Optical Absorption at Room Temperature," The Journal of Physical Chemistry Letters 1(23), 3316-3322 (2010).

[14] Celebrano, M., Kukura, P., Renn, A. and Sandoghdar, V., "Single-molecule imaging by optical absorption," Nat Photon 5(2), 95-98 (2011).

[15] Siegman, A. E. [Lasers], University Science Books (1986).

[16] Gradnhteyn, I. S. and Ryzhik, I. M., [Table of integrals series and products], Academic Press, New York, 366 (1965).

[17] Petschke, A. and La Rivière, P. J., "Comparison of intensity-modulated continuous-wave lasers with a chirped modulation frequency to pulsed lasers for photoacoustic imaging applications," Biomed. Opt. Express 1(4), 1188-1195 (2010).

[18] Danielli, A., Favazza, C. P., Maslov, K. and Wang, L. V., "Picosecond absorption relaxation measured with nanosecond laser photoacoustics," Applied Physics Letters 97(16), 163701-163703 (2010).

[19] Mellen, R. H., "The thermal-noise limit in the detection of underwater acoustic signals," The Journal of the Acoustical Society of America 24(5), 478 (1952).

[20] Born, M. and Wolf, E., [Principles of Optics], Cambridge University Press (1999).

[21] Fujimoto, B. S., Clendenning, J. B., Delrow, J. J., Heath, P. J. and Schurr, M., "Fluorescence and Photobleaching Studies of Methylene Blue Binding to DNA," The Journal of Physical Chemistry 98(26), 6633-6643 (1994).